Journal of Materials Processing Technology 171 (2006) 68–76
Journal of Materials Processing Technology
www.elsevier.com/locate/jmatprotec

Mechanics of machining of face-milling operation performed using a self-propelled round insert milling cutter

Kaushikkumar M. Patel [1], Suhas S. Joshi *

Department of Mechanical Engineering, Indian Institute of Technology, Bombay, Powai, Mumbai 400076, India

Received 9 June 2004; received in revised form 21 April 2005; accepted 15 June 2005

Abstract

There has been a renewed interest in the technology of rotary tools because of their ability to perform more productive machining and the concurrent evolution of a number of new 'difficult-to-machine' materials. This paper presents an investigation into the application of rotary tools in a face-milling operation. The work involved analysis of cutting forces and chip characteristics, and the development of analytical as well as conceptual models to predict the cutting forces. It was evident that the proposed model predicts cutting force magnitude with a fair accuracy.

Keywords: Face-milling; Rotary tools; Self-propelled tools; Cutting forces; Taguchi method

1. Introduction

The technology of rotary tools is being revisited to explore their application in high productivity machining and machining of newer and 'difficult-to-machine' materials. In rotary tools, a tool of truncated cone shape that can rotate about its axis is used [1]. The rotation of the tool about its axis can be effected by directly connecting it to a drive motor. The tool can also be self-propelled (rotated) by providing an inclination angle to it so that a component of cutting velocity drives the tool. Either way, the rotary motion improves performance of the tool since every time fresh cutting edge is presented to the work material and the edge gets ample time to cool down before coming into action again.

It has been reported that James Napier used rotary tools in turning operation as early as 1865. Rotary tools have been applied in turning, facing, shaping and face-milling operations [2]. Shaw [3] described the driven rotary tool operation. Armarego et al. [2] reported that self-propelled tools in a turning operation produced outstanding improvements in tool-life as compared to the stationary (non-rotary) tools. Iyer and Koenigsberger [4] proposed that the self-generated movement of cutting edge increases the chip flow angle and the effective rake angle. Lei and Liu [5] studied machining of titanium alloys using driven rotary tools. Their study revealed that the driven rotary tools (DRT) could increase tool-life. Chen and Hoshi [6] used rotary tools for machining of SiC whisker-reinforced aluminium composites. They concluded that the rotary carbide tools exhibit superior wear-resistance comparable to the polycrystalline diamond tools. They also reported that rotary tools bear neither built-up edge nor flank build-up, and the radial thrust force on rotary tool is 30–40% lower than that of the fixed circular insert. Joshi et al. [7] demonstrated the feasibility of rotary carbide tools in the intermittent machining of Al/SiCp composites. Ezugwu et al. [8] evaluated wear of self-propelled rotary tools when machining titanium alloy IMI 318. Venkatesh et al. [1] studied the effect of various machining parameters on tool-life, surface finish and the type of chip generated during a face-milling operation performed using a self-propelled round insert face-milling cutter. They found that the machining temperature in rotary tools operation is lower than that of while

* Corresponding author. Tel.: +91 22 2576 7527; fax: +91 22 2572 6875.
E-mail address: ssjoshi@me.iitb.ac.in (S.S. Joshi).
[1] On leave from Department of Mechanical Engineering, Institute of Technology, Nirma University of Science and Technology, Ahmedabad 382 481, India.

0924-0136/$ – see front matter
doi:10.1016/j.jmatprotec.2005.06.046

machining with stationary tools. Dabade et al. [9] analyzed chips and surface finish generated during a face-milling operation using a self-propelled round insert face-milling cutter. They reported that the surface roughness is a function of inclination angle provided to the round inserts. Thus, it is observed that a considerable experimental as well as analytical work has been done to investigate the application of rotary tools in turning type operations. However, there is very limited understanding of rotary tools in plain surface generation process like milling [1,9].

This work is a continuation of the earlier work by Dabade et al. [9] in which, self-propelled round inserts were used in a face-milling operation. In this paper, mechanics of face-milling operation performed using self-propelled round insert face-milling cutter is analyzed using statistically designed experiments. An analytical model to predict cutting forces based on an earlier cutting force prediction model for the conventional face-milling operation with stationary tools is proposed.

2. Experimental set-up

A face-milling cutter with self-propelled round inserts fabricated for this experimentation is shown in Fig. 1 [9]. It consists of five rotating inserts mounted at different inclination angles. Fly cutting operation was performed with only one insert mounted on it at the desired inclination angle. The three force components viz., cutting, feed and thrust were measured during the face-milling operation performed with this cutter. A three-component (Model: KISTLER 9257A) dynamometer platform was used to measure cutting forces. The force data were recorded by a specifically designed, very compact multi-channel microprocessor controlled data acquisition system with a single A/D converter preceded by a multiplexer (see Fig. 2). The individual analog signals were first amplified and conditioned by charge amplifier (Model: KISTLER 5006). After amplification and conditioning, the output signals were applied to a multiplexer. Further, they are converted into digital signals by the A/D converter sequentially. The system consists of a sample-hold circuit, which enables it to hold the analog signals till conversion of previous analog to digital data takes place in the A/D converter. When the conversion is complete, the status line from the converter causes S/H to return to the sample mode and acquire signal from the next channel. On completion of acquisition, either immediately or upon receiving a command, the S/H is switched to hold mode. The conversion begins again and the multiplexer switches to the subsequent channel. The data thus obtained can be stored into a memory element for further processing or displayed onto a display device. The data can also be stored on to a personal computer after completion of experiments.

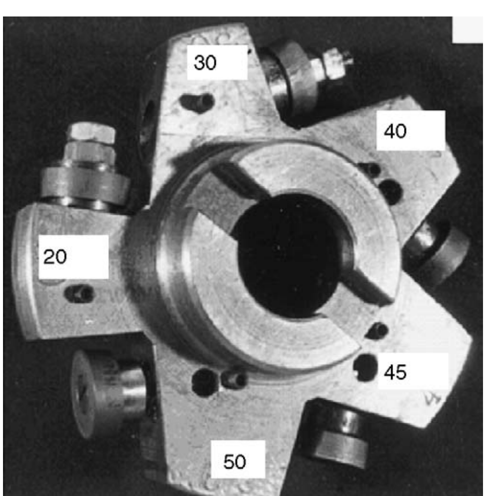

Fig. 1. Self-propelled face-milling cutter with round inserts at various inclination angles [9].

3. Design of experiments and procedure

3.1. Design of experiment

It involves selection of response variables, independent variables, their interactions and an orthogonal array. There were three response variables each corresponding to the maximum magnitude of cutting, feed and thrust component of forces produced during the face-milling operation. Various control parameters, their levels, interactions and degrees of freedom (DOF) chosen for this experiment are given in Table 1.

It is well known from the theory of design of experiments that the selection of an interaction is important to avoid confounding (mixing) of factor effects and to minimize the number of experiments [10]. From the available literature, understanding of physics of the cutting process and the past experience, it was felt that of four independent factors, inclination angle, cutting speed, feed-rate may interact with each other by influencing either the speed of rotary insert or area of undeformed chip cross-section. As observed from the logic presented in Fig. 3, the inclination angle might influence the speed of insert rotation and area of undeformed cross-section whereas, the cutting speed and feed rate may influence the speed of insert rotation and area of chip cross-section respectively. Therefore, interactions between only these factors were considered in this analysis. The degree of freedom of this experiment is 20 (see Table 1) hence a L27 orthogonal array was selected for this experimentation.

3.2. Experimental procedure

Experiments were performed as per the design details mentioned above using the self-propelled round insert face-milling cutter on a vertical milling machine (BFW make). The work piece material used was rolled aluminium (Al 1100) plates of size 160 mm × 14 mm × 10 mm. In all, 54 experiments (including one replication) were performed. Measure-

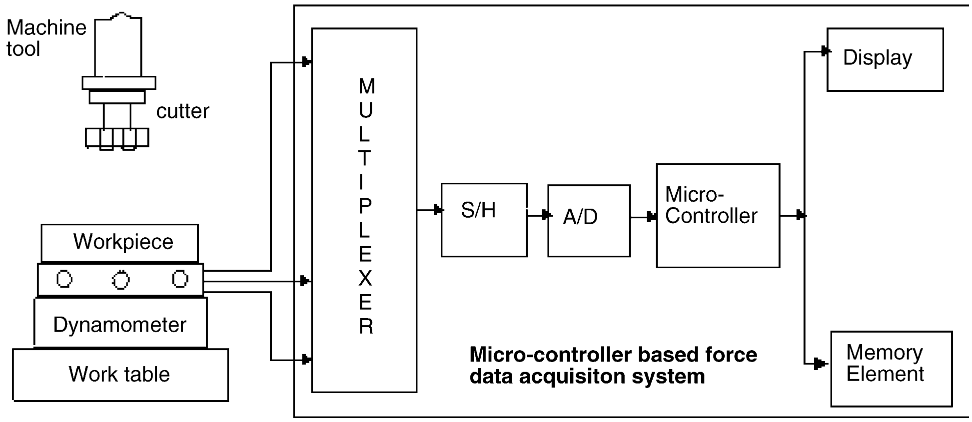

Fig. 2. Multi-channel analog multiplexed force data acquisition system.

Table 1
Control parameters, their levels and interactions

Parameter/interactions	DOF	Level		
		1	2	3
A: Inclination angle (°)	2	30	40	50
B: Cutting speed (m/min)	2	25.44	35.44	70.68
C: Feed rate (mm/min)	2	125	200	250
D: Depth of cut (mm)	2	0.5	1.0	1.3
Interactions AB, AC, BC	$[(3-1)\times(3-1)]\times 3=12$			
Total DOF	20			

ment of cutting forces was carried out using the experimental set-up specifically developed for this purpose. The force data were acquired at the rate of 100 data points per second only after the entire diameter of cutter was engaged with workpiece. In the analysis, an average of twenty data points in a descending order was used to evaluate the maximum force. The maximum magnitudes of F_x, F_y and F_z force components were used as response variables in this analysis [11].

4. Results and discussion

Statistical analysis of experimental result involved analysis of means (AOM) and analysis of variance (ANOVA) using STATGRAPHICS-PLUS software.

4.1. Statistical results and discussion

Mean tables and plots provide variation in a response variable as independent variables change from levels 1 to 3. In the discussion of results here, only the means plots are presented (see Figs. 4–6) whereas, the response tables and ANOVA tables are available elsewhere [12].

It is known that ANOVA helps in formally testing the significance of independent variables and their interactions by comparing the mean square against an estimate of the experimental errors at specific confidence levels. In the analysis, F-ratio is a ratio of mean square error to residual, and is traditionally used to determine significance of a factor. However, F-ratio does not indicate the extent of deviation in the results, therefore P-value called as level of significance [13] is used. If the P-value for a factor is less than 0.05, then the factor is considered as statistically significant at 95% confidence level. It is evident from the analysis of variance (ANOVA) that the magnitudes of maximum cutting force as well as feed forces are significantly influenced (at 95% confidence level) by the inclination angle, cutting speed, feed rate and depth of cut. Whereas, the magnitude of maximum thrust force was significantly influenced by inclination angle and depth of cut. In the following sections, these effects are discussed in detail.

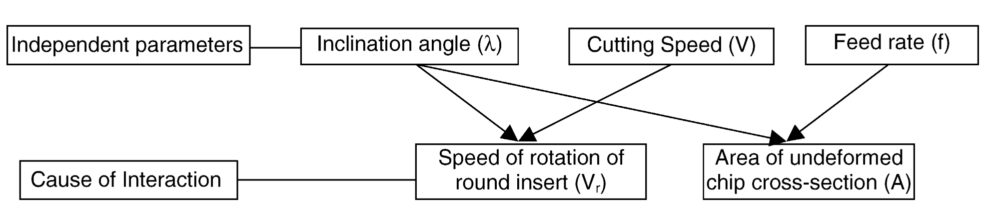

Fig. 3. Selection of interactions.

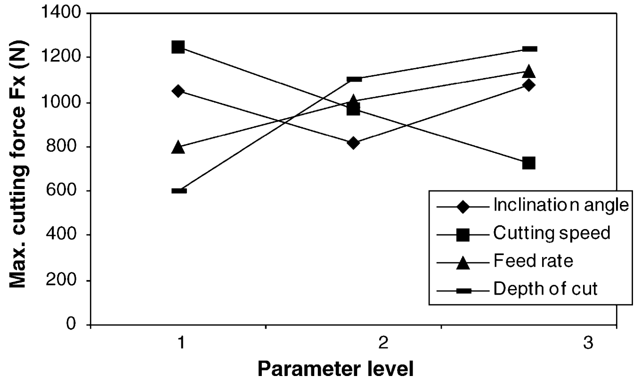

Fig. 4. Mean effect plots for cutting forces F_x.

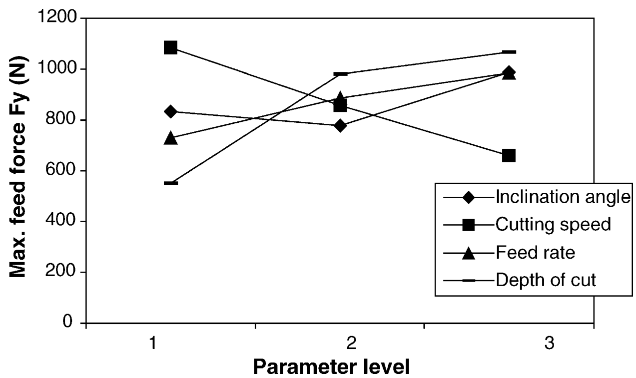

Fig. 5. Mean effect plots for feed forces F_y.

4.1.1. Effect of inclination angle

As the inclination angle changes from 30° (level 1) to 40° (level 2), there is a significant decrease in the magnitude of F_x. On the other hand, a significant increase in F_x is observed when the inclination angle changes from 40° (level 2) to 50° (level 3) (see Fig. 4). Similarly, variation in feed and thrust forces also shows more or less the similar trend (see Figs. 4 and 5). This could be due to an increase in the effective rake angle with an increase in the inclination angle and combined effect of shear and frictional energies per unit volume. Further, a decrease in the shear energy per unit volume with an increase in inclination angle could be due to an increase in the effective rake angle and consequent increase in the shear plane angle in machining. At the same time, the frictional energy remains more or less constant up to an inclination angle of 45°.

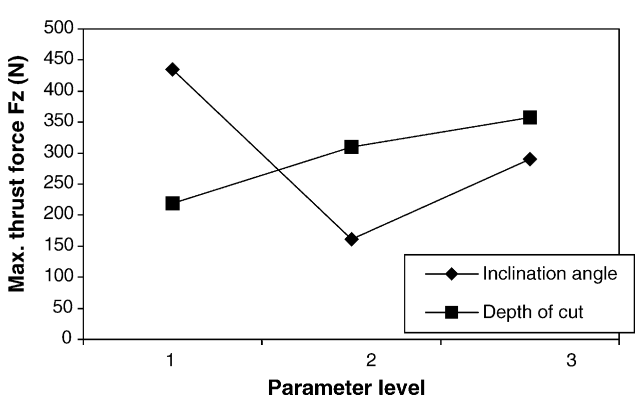

Fig. 6. Mean effect plots for thrust forces F_z.

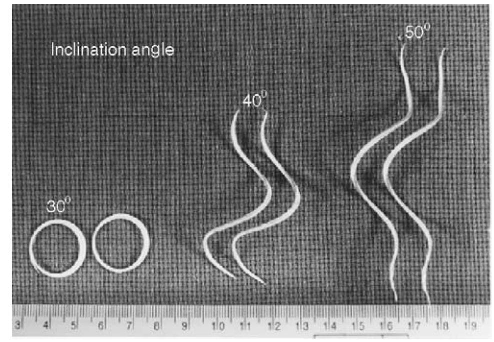

Fig. 7. Photographs of chips produced during self-propelled round insert face-milling operation at different inclination angles. Feed rate 200 mm/min, depth of cut 0.5 mm.

An increase in the magnitude of cutting forces as the inclination angle changes from 40° to 50° could be due to an excessive curling and straightening of chips (see photograph of chips in Fig. 7). Also, cross-section of the chips show an excessive deformation and hence the magnitude of cutting force could increase as the inclination angle changes form 40° to 50°. It is understood that the lowest magnitude of cutting force would occur at 45° inclination angle and thereafter any further increase in the inclination angle would reverse the rake and flank surfaces. It causes a significant increase in frictional energy causing excessive material deformation and consequent increase in the cutting forces [3].

4.1.2. Effect of cutting speed, feed rate and depth of cut

As observed from Figs. 4 and 5, the cutting speed (v) influences the magnitude cutting and feed force components significantly. The magnitudes of both the force components decrease with an increase in the cutting speed. This could be due to thermal softening of the material and decrease in the shear plane angle with an increase in the cutting speed [14].

The feed rate (f_t) influences both cutting force and feed force components significantly. An increase in the maximum cutting and feed forces with increasing feed rate is analogous to the traditional relationship during machining with stationary tools. It could be due to an increase in the cross-sectional area of the uncut chip as shown in Fig. 8.

Depth of cut (f) is the fourth factor which significantly influences the magnitude of cutting, feed and thrust forces; see Figs. 4–6, respectively. It could be due to an increase in the area of undeformed chip cross-section with an increase in the depth of cut. The result is further elaborated by the concept shown in Fig. 9. If the area of chip cross-section assumed to be approximately triangular, at a given feed rate, an increase in the depth of cut from 0.5 to 1.0 mm and from 1.0 to 1.3 mm leads to an increase in cross-sectional area by 231% and 41.90%, respectively. Correspondingly, percentage increases in cutting force is 84.17% and 12.31%, respectively. Thus,

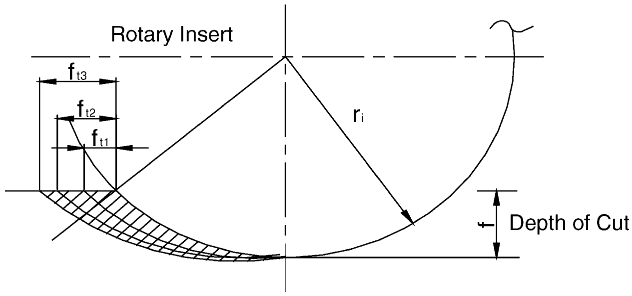

Fig. 8. Model to demonstrate the effect of feed rate the hip cross-section area.

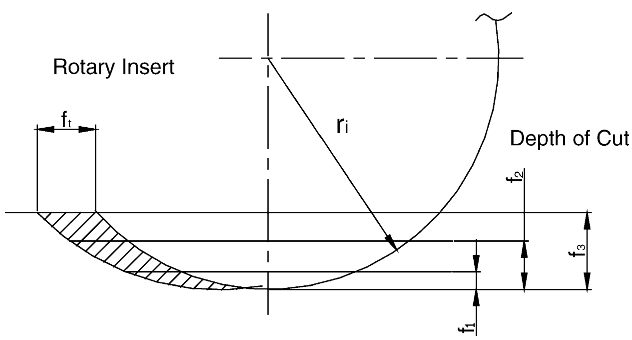

Fig. 9. Model to demonstrate the effect of depth of cut on the chip cross-section area.

increase in cutting force is proportional to an increase in the area of undeformed chip cross-section. Further, an increase in feed and thrust forces could be explained by the similar reasoning.

5. Multiple regression models

In the empirical approach, prediction of magnitude of cutting forces was done based on the regression analysis of the experimental data. A statistical model gives relationship between response variables and four independent parameters such as inclination angle, cutting speed, feed rate and depth of cut. Three models obtained using the multiple linear regressions are

$$\text{maximum cutting force}: F_x(\mathrm{N}) = 92.42 + 1.33\lambda - 10.30v + 2.71f_t + 822.95f \qquad (1)$$

$$\text{maximum feed force}: F_y(\mathrm{N}) = -88.17 + 7.70\lambda - 8.40v + 2.05f_t + 666.79f \qquad (2)$$

$$\text{maximum thrust force}: F_z(\mathrm{N}) = 355.70 - 7.19\lambda - 1.55v + 0.69f_t + 174.09f \qquad (3)$$

where, λ is the inclination angle, v the cutting speed, f_t the feed rate and f is the depth of cut. The predicted values of F_x, F_y and F_z for various experimental runs were compared with the respective experimental values. The R-squared statistics indicates that the multiple regression models as fitted explain 67.6678% of the variability in F_x, 69.1772% in F_y and 27.09% in F_z. The relatively large error in the prediction of maximum thrust force could be due to the inherent inability of the cutter in maintaining constant depth as a result of its rotation and insufficient tool mounting stiffness. Also, some variation could be attributed to the variation in the flatness of the rolled aluminium plates used as workpiece in this experimentation.

6. Analytical modeling of cutting forces

The cutting force system in face-milling has been extensively studied in the past both analytically and empirically [15–22]. Ruzhong and Wang [15] simulated milling forces by combining single tooth orthogonal cutting forces. Koenigsberger and Sabberwal [16] investigated the cutting force pulsations for both slab and face-milling operations using dynamometers. Fu et al. [17] developed a more complex model by taking into consideration cutter geometry, workpiece profiles, cutter run-out effect, etc. in a face-milling operation. Kim and Ehmann [18] considered both static and dynamic forces in their modeling attempt. Young et al. [19] showed how orthogonal theory can be applied to predict cutting forces in face-milling from the knowledge of work material properties and cutting conditions. Lin and Yang [20] used a relationship between flank wear and average cutting force coefficients to estimate the tool wear. Adolfsson and Stahl [21] showed that there are variations in cutting forces between the teeth on a face-milling body. Gu et al. [22] explained model for prediction of static cutting forces in face-milling by including the complex workpiece geometry, multiple pass machining, and effect of machine set-up error.

In the present work, a model for the prediction of cutting forces in a face-milling operation with stationary tools proposed by Kim and Ehmann [18] is used as a base model. The model is adopted to predict forces in a face-milling operation with (rotary) self-propelling inserts by incorporating appropriate

- changes in the geometry of the two cutting operations viz., face-milling with stationary and rotary inserts;
- changes in the area of chip cross-section due to changes in the tool geometry;
- changes in the force magnitudes due to insert rotation.

In the following sections, evolution of the model to predict cutting forces in a face-milling operation is described. Appropriate changes resulting due the first two factors are introduced in the model whereas, the last factor related to the rotation of the rotary insert has not been considered in this analysis due to prevailing complexities in their incorporation.

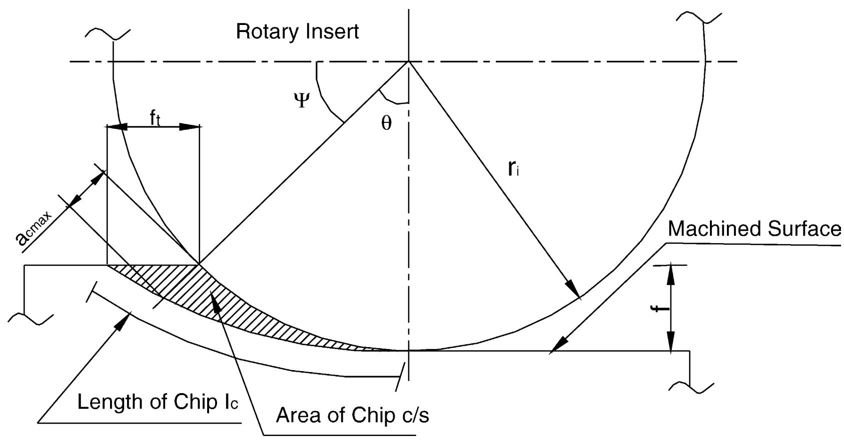

Fig. 10. Geometry of chip in rotary inserts.

6.1. Consideration to the tool geometry

Based on the analogy between the face-milling operation performed using a stationary and rotary inserts, it is understood that the axial rake on a stationary insert is analogous to the rake angle on the rotary insert. Since the rotary inserts have zero degree rake angle, the axial rake in the present calculation is taken as zero. The radial rake on a stationary insert fixed on face-milling cutter is akin to the inclination angle on a rotary insert. Similarly, the lead angle on stationary insert is angle between the direction of the feed motion and the cutting edge. In the case of rotary inserts, it corresponds to the angle between a tangent to the round cutting edge and the direction of feed.

6.2. Consideration to chip cross-sectional area

It is understood that the geometry of an instantaneous chip cross-section produced in the rotary insert face-milling operation is analogous to the longitudinal cross-section of a chip produced in a plunge grinding operation. It is evident from Fig. 10 that the length of chip in a plunge grinding operation is akin to the width of chip $a_{\mathrm{w\,max}}$ in the rotary insert face-milling operation. Therefore, we get the length of chip as

$$l_{\mathrm{c}} = \frac{d_i}{2}\sin(\theta) \tag{4}$$

where, d_i is the diameter of the round insert and

$$\cos(\theta) = \frac{(d_i/2) - f}{d_i/2} = 1 - \frac{2f}{d_i} \tag{5}$$

where, f is the depth of cut.

After substituting Eq. (5) in the following relationship, we get

$$\sin^2(\theta) = 1 - \cos^2(\theta) = \frac{4f}{d_i} - \frac{4f^2}{d_i^2} \tag{6}$$

Substituting Eq. (6) in Eq. (4) and neglecting the second order term, we get

$$l_{\mathrm{c}} = (fd_i)^{0.5} = a_{\mathrm{w\ max}} \tag{7}$$

It is further observed that the actual width of chip $a_{\mathrm{w\ max\ actual}}$ is related to maximum width of chip by the inclination angle, λ as shown in Fig. 11 and is given by

$$a_{\mathrm{w\,max\,actual}} = \frac{a_{\mathrm{w\,max}}}{\cos(\lambda)} \tag{8}$$

In a self-propelled face-milling cutter, the diameter of round insert is analogous to the diameter of grinding wheel. Therefore, the maximum thickness of chip $a_{\mathrm{c\,max}}$ can be related to the feed as shown in Fig. 11 by

$$a_{\mathrm{c\,max}} = f_t\ \sin(\psi) \tag{9}$$

where, $\sin(\psi) = \frac{r_i - f}{r_i}$, r_i is the radius of the insert.

It is known that the volume of a typical chip in a plunge grinding operation is given by [23]

$$V = \frac{1}{6}a_{\mathrm{w\ max}}a_{\mathrm{c\ max}}l_{\mathrm{c}} \tag{10}$$

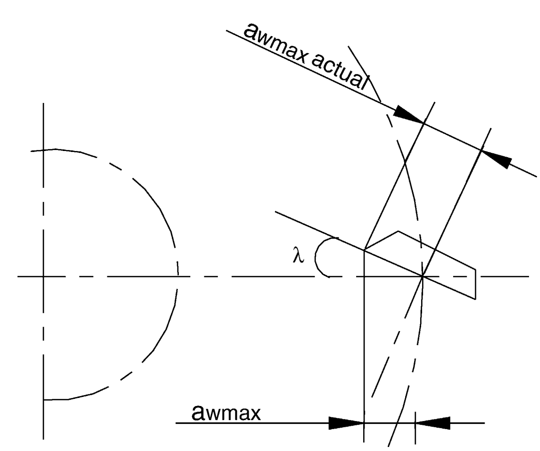

Fig. 11. Effect of insert inclination angle on self-propelled face-milling.

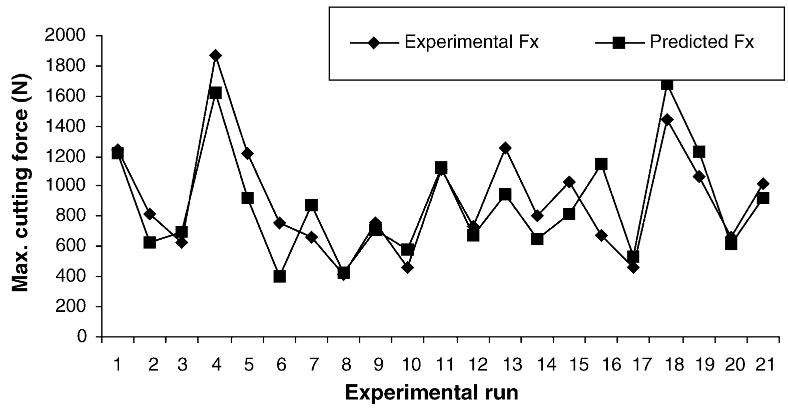

Fig. 12. A comparison of predicted and experimental magnitude of F_x.

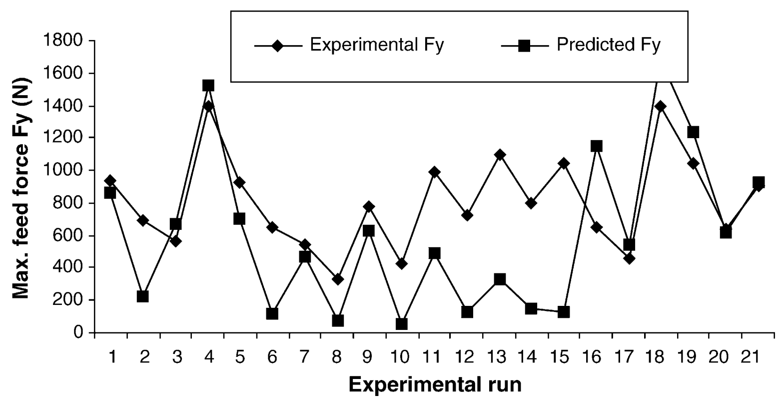

Fig. 13. A comparison of predicted and experimental magnitude of F_y.

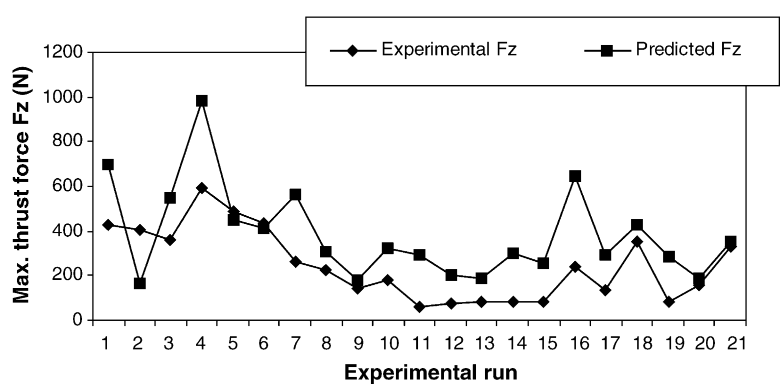

Fig. 14. A comparison of predicted and experimental magnitude of F_z.

Therefore, based on the analogy, the area of a typical chip for the *i*th insert at any angle ϕ is given by

$$A_i(\phi) = \frac{1}{6} a_{\mathrm{c}\,max} a_{\mathrm{w}\,max\,\mathrm{actual}} \tag{11}$$

By substituting value of $a_{\mathrm{w\ max\ actual}}$ and $a_{\mathrm{c\ max}}$ in Eq. (11) we get,

$$A_i(\phi) = \frac{1}{6} f_t \sin(\psi) \frac{(fd_i)^{0.5}}{\cos(i)} \tag{12}$$

Many authors [15,17,18] have proposed that the tangential force, $F_{\mathrm{T}}(i,\phi)$ (i.e. the tangential force acting on a tooth i at an angle ϕ) a tooth can be expressed as the product of the chip cross-sectional area, $A_i(\phi)$, and of the specific cutting pressure K_{T}. The radial force, $F_{\mathrm{R}}(i,\phi)$, acting along the cutting edge in the radial direction of the cutter is obtained by multiplying the tangential force by empirical constant K_{R}. Neglecting effects of rake and inclination angles, relationships for the evaluation of tangential and radial force during a face-milling operation can be given by [15,17,18]

$$\text{tangential force } F_{\mathrm{T}}(i,\phi) = K_{\mathrm{T}} A_{\mathrm{i}}(\phi) \tag{13}$$

radial force $F_R(i, \phi) = K_R F_T(i, \phi)$ (14)

axial force $F_A(i, \phi) = K_A F_T(i, \phi)$ (15)

where K_T is a specific cutting pressure, K_R a dimensionless constant relating radial force to tangential force and K_A is a ratio of the axial to tangential force. Therefore, the instantaneous X-, Y- and Z- force components at the cutter rotation angle ϕ for a fly cutter (with only one insert on it) are functions of $A_i(\phi)$ and are given by

$$F_x(i, \phi) = F_T(i, \phi)\sin(\theta_i(\phi)) - F_R(i, \phi)\cos(\theta_i(\phi)) \quad (16)$$

$$F_y(i, \phi) = F_T(i, \phi)\cos(\theta_i(\phi)) + F_R(i, \phi)\sin(\theta_i(\phi)) \quad (17)$$

$$F_z(i, \phi) = F_A(i, \phi) \quad (18)$$

6.3. Comparison with the experimental results

It is known that in one revolution of the cutter, the area of chip cross-section varies from zero at the beginning (at θ_i $(\Phi) = 0^\circ$) to maximum (at θ_i $(\Phi) = 90^\circ$). Therefore, the maximum area of cross-section at θ_i $(\Phi) = 90$ was evaluated using Eq. (12) along with the constants. Thus, the magnitudes of peak forces in X-, Y- and Z-direction were evaluated. Similarly, the magnitude of peak forces was also obtained from the experimental data. A comparison of peak forces as evaluated using models (Eqs. (16–18)) and the corresponding experimental values is presented in Figs. 12–14. The average error between experimental and predicted magnitude of F_x, F_y and F_z was found to be 18.86%, 43.17% and 47.75%, respectively. It can be observed from the plot that by and large predicted values of X-, Y- and Z- components of force follow the similar trend as that of the corresponding trends in the experimental values. The relatively higher variation in the predicted magnitudes of F_y and F_z could be due to the rotation of insert being not taken into account and the inherent uncertainty in the rotary spindle stability.

7. Conclusions

1. Cutting forces were measured using a micro-controller based force measurement system in a face-milling operation performed using a face-milling cutter with self-propelled round inserts. An orthogonal array (L27) based design of experiments was adopted to evaluate the four main factor effects and three 2-factor interactions.
2. It was evident that magnitudes of all forces (cutting, feed and thrust) decrease with increasing inclination angle up to 45° and increase thereafter. Initial decrement in forces up to 45° inclination angle could be due to an increase in the effective rake angle with an increase in the inclination angle. In addition, a decrement in the shear energy and constant nature of frictional energy also contributes to this effect. When the inclination angle increases beyond 45°, it causes reversal of rake and flank surfaces thereby excessive material deformation takes place. This may result in an increase in the forces (cutting, feed and thrust) with an increase in the inclination angle.
3. A reduction in the magnitude of cutting and feed forces with an increase in cutting speed could be due to the thermal softening of material, thereby the reduction in the co-efficient of friction and increase in shear plane angle. Similarly, the increment in all the forces with depth of cut could be due to an increase in area of undeformed chip cross-section. The cutting force and feed force also increase with the feed rate, which could be also due to an increase in the cross-sectional area of undeformed chip.
4. The analytical model proposed in this work by incorporating appropriate changes in the tool geometry and area of undeformed chip cross-section in the model for the face-milling operation with stationary tools gives fairly accurate prediction of F_x. The relatively higher variation in the predicted magnitudes of F_y and F_z could be due to the rotation of insert being not taken into account and uncertainty in rotary spindle stability.

References

[1] V.C. Venkatesh, S. Rajesham, V. Kamala, Wear and surface finish in face-milling with rotary inserts, in: Proceedings of Fifth AIMTDR conference, 1972, pp. 183–190.
[2] E.J.A. Armarego, V. Karri, A.J.R. Smith, Fundamental studies of driven and self-propelled rotary tool cutting process—I theoretical investigation, Int. J. Mach. Tool Manuf. 34 (6) (1994) 785–801.
[3] M.C. Shaw, Metal Cutting Principles, first ed., C B S Publication and Distributors, India, reprint 1992, pp. 481–486.
[4] N.R. Iyer, F. Koenigsberger, Experiments with self-propelled rotary cutting tools, in: Proceedings of Ninth IMTDR Conference, 1968, pp. 945–959 (part 2).
[5] S. Lei, W. Liu, High speed machining of titanium alloys using the rotary tool, Int. J. Mach. Tools Manuf. 42 (6) (2002) 653–661.
[6] P. Chen, T. Hoshi, High performance machining of SiC whisker-Reinforced aluminium composite by self-propelled rotary tools, Ann. CIRP 41 (1) (1992) 59–62.
[7] S.S. Joshi, N. Ramkrishnan, H.E. Nagarwalla, P. Ramkrishnan, Wear of rotary carbide tools in machining of Al/SiCp composites, Wear 230 (2) (1999) 124–132.
[8] E.O. Ezugwu, K.A. Olajire, Z.M. Wang, Wear evaluation of a self-propelled rotary tool when machining titanium alloy IMI, 318, Proc. Inst. Mech. Eng, Part B, J. Eng. Manuf. 216 (2002) 891–896.
[9] U.A. Dabade, S.S. Joshi, N. Ramakrishnan, Analysis of surface roughness and chip cross-sectional area while machining with self-propelled round insert milling cutters, J. Mater. Process. Technol. 132 (1–3) (2003) 305–312.
[10] J. Ross Phillip, Taguchi Techniques for Quality Engineering, Edition, McGraw-Hill Book Company, New York, 1988.
[11] K.M. Patel, S.S. Joshi, D.V. Bhoir, Cutting forces in machining using self-propelled round inserts face-milling cutter, in: Proceedings of international Conference on CAD, CAM, Robotics and Autonomous factories, 2003.
[12] K.M. Patel, Mechanics of Machining Using Self-Propelled Round Insert Milling Cutter, M.Tech. Dissertation, Indian Institute of Technology, Mumbai, India, May 2003.
[13] D.C. Montgomery, Design and Analysis of Experiments, fourth ed., John Wiley & Sons Publication, New York, 1996.
[14] M. Alauddin, M. El baradi, M.S.J. Hashmi, Cutting Forces in the End Milling of Inconel 718, J. Mater. Process. Technol. 77 (1998) 153–159.

[15] Z. Ruzhong, K. Wang, Modeling of cutting forces pulsation in face-milling, Ann. CIRP 32 (1) (1983) 21–26.
[16] F. Koenigsberger, A.J.P. Sabberwal, An investigation into the cutting force pulsation during milling operations, Int. J. Mach. Tool Des. Res. 1 (1961) 15–33.
[17] H.J. Fu, R.E. Devor, S.G. Kapoor, A mechanistic model for prediction of the force system in face-milling operations, Trans. ASME, J. Eng. Ind. 106 (1984) 81–88.
[18] H.S. Kim, K.F. Ehmann, A cutting force model for face-milling operations, Int. J. Mach. Tools Manuf. 33 (5) (1993) 651–673.
[19] H.-T. Young, P. Mathew, P.L.B. Oxley, Predicting cutting forces in face-milling, Int. J. Mach, Tools Manuf. 34 (6) (1994) 771–783.
[20] S. Lin, R. Yang, Force based model for tool wear monitoring in face-milling, Int. J. Mach. Tools Manuf. 35 (9) (1994) 1201–1211.
[21] C. Adolfsson, J.E. Stahl, Cutting force model for multi-toothed cutting processes and force measuring equipment for face-milling, Int. J. Mach. Tools Manuf. 35 (12) (1995) 1715–1728.
[22] F. Gu, S.G. Kapoor, R.E. Devor, P. Bandyopadhyay, An enhanced cutting force model for variable face-milling with variable cutter feed motion and complex workpiece geometry, Trans. ASME, J. Eng. Ind. 119 (1997) 467–475.
[23] G. Boothroyd, W.A. Knight, Fundamentals of Machining and Machine Tools, Marcel Dekker, NY, 1989, p. 288.